1995ApJ...444..582D

THE ASTROPHYSICAL JOURNAL, 444:582–589, 1995 May 10
© 1995. The American Astronomical Society. All rights reserved. Printed in U.S.A.

DIFFUSE HOT GAS IN THE NGC 4261 GROUP OF GALAXIES

DAVID S. DAVIS[1,2]
Astronomy Department, University of Maryland, College Park, MD 20742
RICHARD F. MUSHOTZKY
Laboratory for High Energy Astrophysics, Goddard Space Flight Center Greenbelt, MD 20771
JOHN S. MULCHAEY[3]
Space Telescope Science Institute, 3700 San Martin Drive, Baltimore, MD 21218
D. M. WORRALL AND M. BIRKINSHAW
Harvard-Smithsonian Center for Astrophysics, 60 Garden Street, Cambridge, MA 02138
AND
DAVID BURSTEIN
Department of Physics and Astronomy, Arizona State University, Tempe, AZ 85287-1504
Received 1994 May 23; accepted 1994 November 11

ABSTRACT

We have found diffuse X-ray gas in the group of galaxies containing the elliptical galaxy NGC 4261. This galaxy along with its associated companions are behind the Virgo cluster in the W-cloud. A recent analysis of the velocity structure in the Virgo region indicates that the W-cloud has ~ 30 members, most of which are low luminosity dwarfs. The hot X-ray emitting gas is centered about halfway between NGC 4261 and NGC 4264 and extends out to a radius of $\sim 40'$ (620 kpc). The spectral data for the diffuse component are well fitted with a Raymond-Smith plasma model with a temperature of $0.85^{+0.21}_{-0.16}$ keV and abundance < 0.08 times the solar value. Under the assumption that the diffuse gas is in hydrostatic equilibrium the total mass within $40'$ is $1.9 \times 10^{13}\ M_{\odot}$. We estimate that the total baryonic mass of the hot gas and the galaxies is 20%–34% of the total mass in the central $40'$ radius of this group. This group of galaxies contains NGC 4273 which exhibits a "bow shock" morphology similar to that of NGC 2276. This is thought to occur when the ram pressure from the intragroup gas significantly perturbs the interstellar medium in a late-type galaxy. We show that this is unlikely in this group.

Subject headings: galaxies: clusters of — galaxies: individual (NGC 4261, NGC 4264, NGC 4273) — intergalactic medium — X-rays: galaxies

1. INTRODUCTION

The detection of hot X-ray emitting gas in the NGC 2300 group, a very poor group of galaxies (Mulchaey et al. 1993) and the detection of hot gas in compact groups (Biermann, Kronberg, & Madore 1982; Biermann & Kronberg 1983; Bahcall, Harris, & Rood 1984; Ponman & Bertram 1993) established both that these systems are massive enough to retain hot X-ray-emitting gas, and that this gas is a significant fraction of the baryonic mass. In three groups (NGC 2300 [Mulchaey et al. 1993; Hickson 1982]; Compact Group 62 (HCG 62), observed by Ponman & Bertram [1993]; and the NGC 5044 group [David et al. 1994]) enough photons are collected by the Position Sensitive Proportional Counter (PSPC) of *ROSAT* that the physical properties of the hot gas are relatively well determined. Under the assumption that the hot gas is in hydrostatic equilibrium with the gravitational potential of the group, the total mass of the group can be measured. The fraction of baryonic mass contained in the luminous matter, in both the galaxies and the hot gas, is $\sim 6\%$ for the NGC 2300 group, greater than 13% for HCG 62 and 12% for the NGC 5044 group. Hence, the conclusion is drawn that up to 95% of the gravitating matter in these groups is dark. These three groups also share relatively low X-ray temperatures (0.8–1.2 keV) and the NGC 2300 group and HCG 62 have low metal abundance (6%–15% of solar) while the NGC 5044 group has a metal abundance close to solar. Both the low metal abundance and high ratio of dark matter to baryonic matter in two of these groups distinguish them from clusters that have been studied through X-ray observations of hot gas.

The NGC 2300 group was chosen for observation because it contained a spiral galaxy (NGC 2276) thought to be undergoing ram-pressure stripping (Mulchaey et al. 1993). As part of the ongoing program of four of us (DSD, RFM, JSM, DB) to study the X-ray properties of small groups of galaxies, we examined the *ROSAT* archives for other observations that coincided with groups containing similar-appearing galaxies. Such a group is the NGC 4261 group, which contains, at its periphery, NGC 4273, a galaxy of similar morphological appearance to NGC 2276. The *ROSAT* observation of this group was obtained by two of us (M. B. and D. M. W.) to study the X-ray emission from the giant elliptical and active galaxy. NGC 4261. Together we realized that, if the NGC 4261 group contains diffuse hot gas, we have the opportunity to examine how the diffuse gas relates to the hot gas contained within the gravitational well of the giant elliptical itself. The result of this co-investigation is the present paper.

Section 2 details the *ROSAT* X-ray observations of NGC 4261 and the data analysis that was necessary to search for low surface brightness gas in this group. Diffuse hot gas is found in

[1] Also at Laboratory for High Energy Astrophysics, Goddard Space Flight Center.
[2] Present Address: Department of Physics and Astronomy, University of Alabama.
[3] Also at Department of Astronomy, University of Maryland.

© American Astronomical Society • Provided by the NASA Astrophysics Data System

1995ApJ...444..582D

the NGC 4261 group, and we analyze its physical properties in § 3, both in terms of the diffuse gas itself, and its relationship with the hot gas more centrally concentrated around the giant elliptical itself.

The NGC 4261 group lies in the direction of the Virgo cluster on the sky but at approximately twice the redshift of the cluster. Nolthenius (1993) studied the complex optical and velocity structures found in the Virgo cluster region and found that the NGC 4261 group is well separated from the Virgo cluster itself. Using the Center for Astrophysics sample of galaxies in the Virgo region and an improved grouping algorithm, Nolthenius assigns 33 galaxies to the NGC 4261 group, and we find that eight of these are within the $\sim 40'$ radius within which we detect X-ray gas. This group has a mean heliocentric radial velocity of 2117 km s^{-1} and has a velocity dispersion of 465 km s^{-1}. Nolthenius (1993) corrects this velocity to obtain a distance using the Virgo–Great Attractor flow model as presented in Faber & Burstein (1988) and obtains a distance of 53 Mpc to this system for an $H_0 = 50$ km s^{-1} Mpc^{-1}. This group is dominated by the elliptical galaxy NGC 4261 which lies near its kinematic center.

2. OBSERVATIONS

The X-ray data were obtained with the *ROSAT* PSPC, which observed the field centered near NGC 4261 for 22042 s. NGC 4261 along with ~ 13 point sources are detected within a radius of 20′ from the center of the field. Most of these point sources are *not* other galaxies in the NGC 4261 group, a result not surprising as most of the other galaxies in the NGC 4261 group are low-luminosity dwarf galaxies and are expected to be weak X-ray sources.

Detection of faint, diffuse emission over a field of view of 1.4 deg^2 is difficult with any astronomical observation, let alone in the PSPC which is subject to a variety of systematic effects (Snowden et al. 1994). In addition to the obvious problems of dealing with observations near the "ribs," other sources of background contamination also exist. In particular, several sources of contamination originate from the near-Earth environment of the satellite. These include charged particle events detected as X-rays by the PSPC and solar X-ray emission scattered off Earth's atmosphere into the optical path of the telescope.

We examine in detail three sources of background contamination: particle events, X-rays from the quiet Sun and X-rays from solar flares. Anticoincidence detectors aboard the spacecraft can reject in excess of 99% of the apparent X-ray detections caused by particle events in the PSPC. However, at times, e.g., when the spacecraft is near the South Atlantic Anomaly, even the small number of events which are accepted as source X-rays can be significant. These times are evident in the Master Veto Rate, which is the number of rejected (particle-generated) X-ray events and the total accepted X-ray event rate. These event rates are supplied with the X-ray data. A simultaneous increase in both the Master Veto Rate and the accepted X-ray event rate indicates that particle events are contaminating the exposure.

X-rays from the quiet Sun and from solar flares can both be scattered from Earth's upper atmosphere and into the telescope's detectors. X-rays from the quiet Sun are usually only a problem near the beginning or the end of an observation period when the target is eclipsed by Earth and the telescope is looking through a relatively large pathlength of Earth's atmosphere. These times are relatively easy to spot as an enhancement in the total accepted X-ray event rate at the beginning and end of each subinterval of data. Scattered X-rays from solar flares can occur at any time during the observation and are also seen as an increase in the total X-ray event rate.

To prepare these data for analysis we first used the accepted X-ray event rates and the Master Veto Rates to screen the data for increased background from various short-term enhancements. A rise in the accepted event rate for the full field usually indicates X-rays of local origin are being detected. To exclude these times we first smooth the accepted event rate, apply a three-point Hanning smoothing to the event rate data provided with the data set, and find the mean and standard deviation for the event rates. We then determine where the accepted event rate deviates more than 2 σ from the smoothed accepted count rate and interactively examine the times when this is occurring. In general these times occur near the beginning or the end of the interval where the automatic processing has excluded some of the data. We exclude times from final data set where the Master Veto Rate exceeds 170 counts s^{-1} and times where the accepted event rate deviates from the mean by more than 2 σ. The net result of this screening process is that we exclude 1760 s of data from the processed image received from the *ROSAT* Science Data Center, resulting in a total exposure time of 20282 s.

A separate source of "contamination" for the analysis of diffuse emission comes from the point sources in the field, including the primary target of this observation, the giant elliptical NGC 4261. The contribution to the diffuse background by point sources is removed by simply excluding a region centered on each source. Using the measured point spread function, we determined that exclusion of a region with a radius of 3′ around each point source was a reasonable compromise for the removal of point source flux from sources with off-axis angle of less than 20′. In this way, greater than 90% of the point source flux is eliminated while not removing too much of surface area from the diffuse cloud. For off-axis angles greater than 20′ larger exclusion radii were used to account for the larger point spread function at greater off axis angles. These larger radii are determined by using analytic fits to off-axis point sources from the ground calibration data for the PSPC.

The final source of "contamination" for our purposes is of local origin, the diffuse emission from our own Galaxy. Much of this emission is thought to be from a $\sim 10^6$ K plasma in the neighbourhood of the Sun. At high galactic latitudes we find that this emission is fairly uniform over the PSPC field of view and, as with the diffuse extragalactic background, removal using data from the same field generally provides a good estimate of the background for an extended source. In addition we restrict our analysis of the data to the energy range between 0.5 and 2.0 keV to minimize the uncertainty from the local soft X-ray background. In the case of the NGC 4261 observation, the background for the spectral analysis is taken from an annular region centered on the peak of the diffuse emission with an inner radius of 40′ and an outer radius of 50′. In adopting this background level, we are being conservative in our estimate of the total flux of the diffuse gas, which could extend beyond the 40′ limit assumed here. If the gas does extend beyond 40′ then our estimate of the baryonic mass of this group is a lower limit.

3. DATA ANALYSIS

Once the data were screened to eliminate the effects discussed above, they were corrected for vignetting using expo-

© American Astronomical Society • Provided by the NASA Astrophysics Data System

1995ApJ...444..582D

sure maps derived for the PSPC (Snowden et al. 1994). The effective exposure maps in the four energy bands above 0.5 keV are generated using software at Goddard Space Flight Center and are based on the precise orientation of the satellite during the observation. Having used these energy-dependent exposure maps to correct for the vignetting, we then co-add the images in the 0.5–2.0 keV energy range. A contour map of the diffuse X-ray emission found by the above analysis is given in Figure 1. As is apparent from the positions of the galaxies relative to the diffuse gas, no galaxy, including NGC 4261, is centered on the gas.

To produce a more quantitative measure of this diffuse emission, we proceeded in several stages. First, we produced radial plots of the surface brightness using the 0.5–2.0 keV band image. The centroid of the diffuse emission is at $\alpha = 12^h19^m27^s$, $\delta = 05°49'58''$ (J2000) and we excluded all detected point sources as described above. We also extracted a radial profile from three test fields to determine if the excess emission in the NGC 4261 field was an instrumental artifact or the result of our analysis method. In no case did we find background variations like those seen in the NGC 4261 field; all other fields were consistent with a flat background. Radial profiles for the NGC 4261 group and a 34 ks observation of a point source (RP 200091), which provides a useful background reference for the NGC 4261 field are shown in Figure 2. We fit the X-ray luminosity distribution of NGC 4261 in Figure 2 using a modified King profile

$$S(r) = S_0[1.0 + (r/a)^2]^{-3\beta+0.5},$$

where S_0 is the central surface brightness, r is the radial distance from the center of the distribution, a is the core radius, and β is a measure of the ratio of kinetic energy in the gas to the kinetic energy in the galaxies (Jones & Forman 1984). *The background was explicitly included in the fit as a constant added to the model.* We found that a King profile fitted the data reasonably well, given the nonspherical contours, with a reduced chi-squared value of 1.5. The background in this observation can be modeled as a constant with a surface brightness of $(4.11 \pm 0.04) \times 10^{-4}$ counts s^{-1} arcmin^{-2} in the 0.5–2.0 keV band (90% confidence error). This determination of the local background is consistent with the background $(3.98 \pm 0.43) \times 10^{-4}$ counts s^{-1} arcmin^{-2} in the 0.5–2.0 keV energy range provided by MPE using low-resolution All Sky Survey data. This agreement between the All Sky Survey and our background determination gives us confidence that our method yields an accurate measure of the background and the

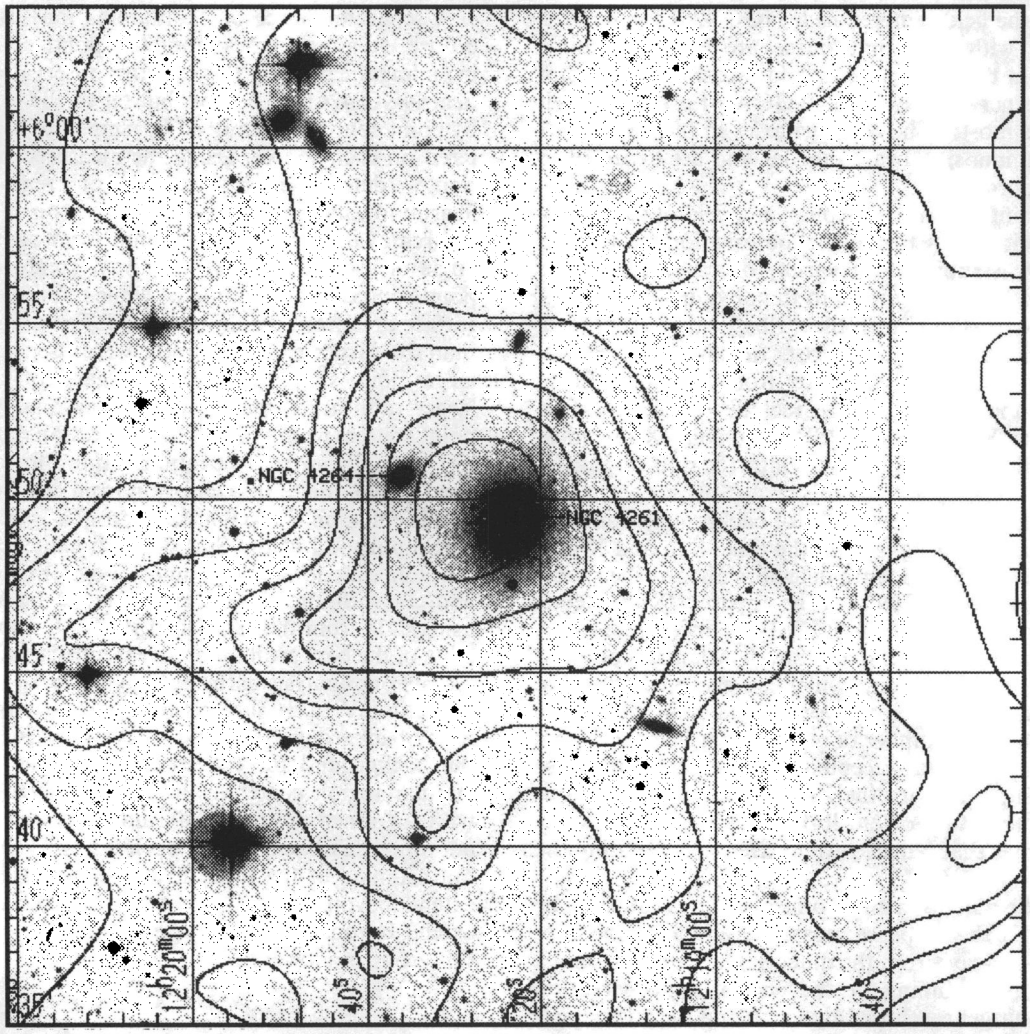

FIG. 1.—The optical image of NGC 4261 with X-ray contours overlaid. The optical image is from the digitized version of the Palomar Observatory Sky Survey Quick *V* plates. Point sources have been removed from the X-ray image and then the data were smoothed with a Gaussian with $\sigma = 1'.5$.

© American Astronomical Society • Provided by the NASA Astrophysics Data System

1995ApJ...444..582D

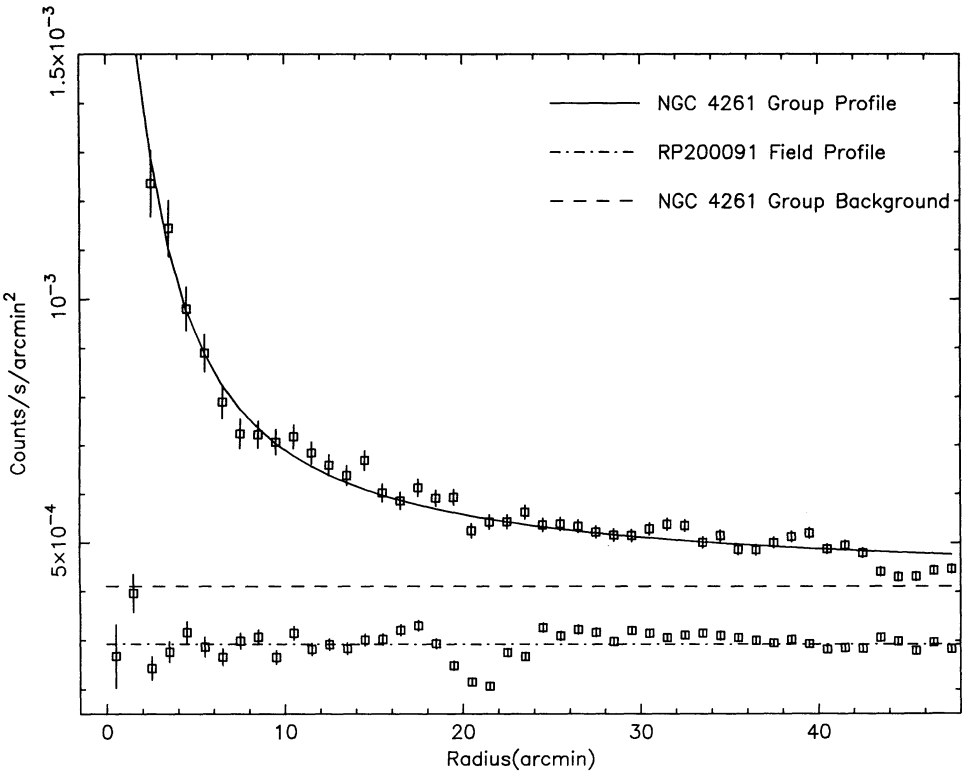

FIG. 2.—The surface brightness profile for NGC 4261 is shown along with the surface brightness profile from a 33 ks observation of a point source. The dip in the lower profile at 20′ is from the PSPC's circular support structure. The excess in the profile for NGC 4261 can be seen to ~40′.

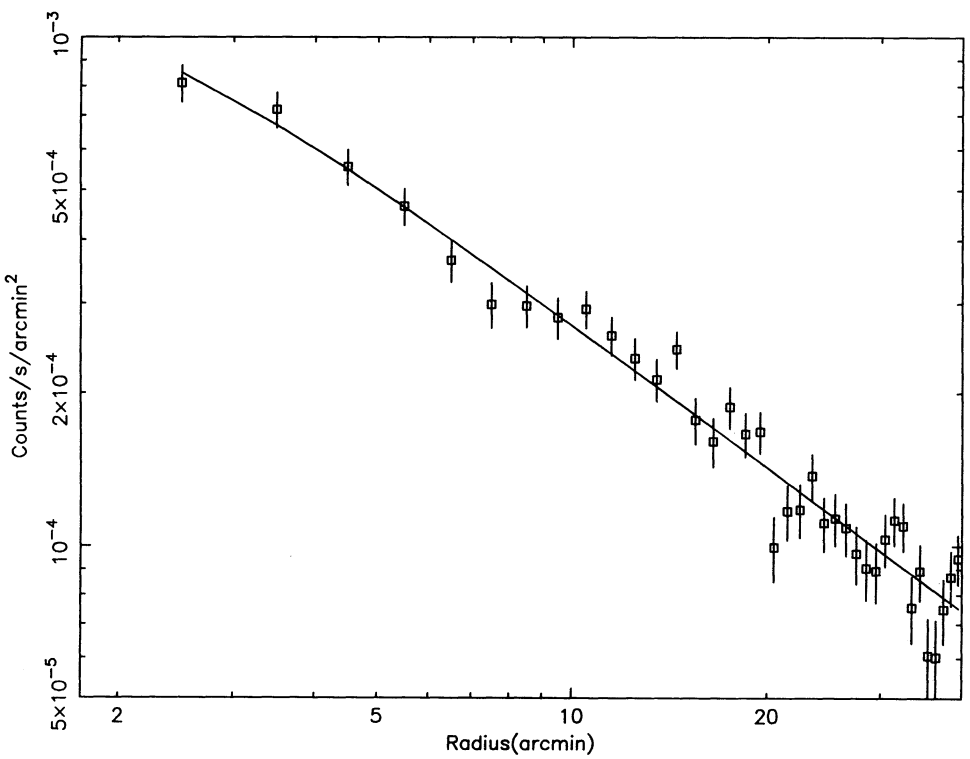

FIG. 3.—The background-subtracted profile for NGC 4261 group is shown here on a log-log plot. The solid line is the best-fit King profile.

© American Astronomical Society • Provided by the NASA Astrophysics Data System

1995ApJ...444..582D

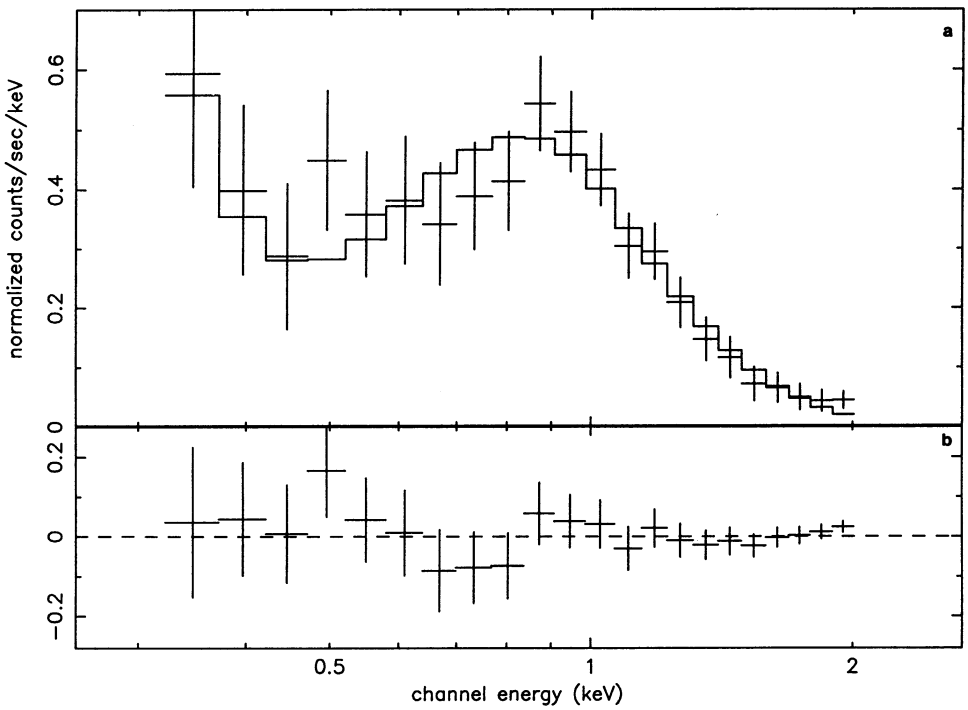

FIG. 4.—(*a*) The X-ray spectrum of the diffuse gas is shown along with the best-fit Raymond-Smith model. (*b*) Residuals of the best-fitting model spectrum and the data.

extended emission. After background subtraction we find the best-fit core radius is $1'.68^{+1.46}_{-0.23}$ (26^{+23}_{-4} kpc) and the central surface brightness is 1.52×10^{-3} counts s^{-1} arcmin^{-2}. The best fit value of β is 0.31 with a 90% confidence range from 0.30 to 0.34 for these fits. The background-subtracted data along with the best-fit model is shown in Figure 3. These data are consistent with the excess emission noted by Worrall & Birkinshaw (1994) in their profile of NGC 4261 when corrected for the different energy range used. The emission associated with NGC 4261 itself, beyond its 3′ radius of exclusion, provides a negligible contribution to the profile in Figure 3.

The spectral data are extracted using an annulus centered at the peak of the diffuse emission and extending from 3′ to 40′ which avoids including the inner extended component seen by Worrall & Birkinshaw (1994). The background region was chosen to be an annulus 40′–50′ from the center of the group emission. Point sources were excluded from the extracted spectrum and background region by eliminating a 3′ radius circle around each source as described previously (§ 3). We fitted a Raymond-Smith plasma model (Raymond & Smith 1977) with galactic absorption fixed at $N_H = 1.87 \times 10^{20}$ cm^{-2} (Stark et al. 1992) and restricted the fitted energy range between 0.35 keV and 2.0 keV. Initially we fix the elemental abundance at 0.3 solar. The derived temperature is $1.07^{+0.19}_{-0.11}$ keV. This model fitted the data with a reduced chi-squared (χ^2_ν) of 1.11 for 21 d.o.f. Fitting these data with the same model but allowing the metal abundance to vary changes the physical parameters of the gas only slightly. The best-fit temperature is $0.85^{+0.21}_{-0.16}$ keV and the metal abundance is 0.02 solar with a 90% confidence range from 0 to 0.08. The spectral data along with the best-fit model are shown in Figure 4*a*, and the residuals to this fit are shown in Figure 4*b*. The emission integral for this fit is 6.27×10^{65} cm^{-5}. Assuming the gas is at the same distance as NGC 4261, its 0.5–2.0 keV luminosity is 5.5×10^{41} ergs s^{-1}. In addition to fitting the spectral data as a whole we also divided the data into three annuli to investigate any variations with radius. The spectra were extracted from 3′ to 13′, from 13′ to 24′, and from 24′ to 40′. We fitted each spectrum with a Raymond-Smith plasma model with the temperature and abundance as free parameters. These fits are consistent with a single-temperature plasma with low metal abundance and show no significant variations with radius. Table 1 summarizes the spectral fits.

TABLE 1

SPECTRAL FITTING RESULTS

kT (keV)	Abundance	N_H (cm^{-2})	χ^2/d.o.f.	Radii
Fit with Fixed Abundance				
$1.07^{+0.19}_{-0.11}$	0.3	1.87×10^{20}	23.3/21	3′–40′
Fits with Variable Abundance				
$0.85^{+0.21}_{-0.16}$	0.00–0.08	1.87×10^{20}	10.1/20	3′–40′
0.82 ± 0.08.....	0.00–0.02	1.87×10^{20}	29.8/20	3′–13′
0.99 ± 0.12.....	0.06–0.40	1.87×10^{20}	14.9/20	13′–24′
0.61 ± 0.15.....	0.00–0.04	1.87×10^{20}	22.3/20	24′–40′

4. DISCUSSION

4.1. *Group Gas*

The discovery of hot X-ray emitting gas in the NGC 2300 group (Mulchaey et al. 1993) showed that at least one small group of galaxies could retain a hot atmosphere. The gas in the NGC 2300 group is cool ($T \sim 1$ keV) and has an extremely low metal abundance, which suggests that this may be primordial gas that has not been enriched by supernovae in the constituent galaxies. HCG 62 (Ponman & Bertram 1993), a compact group with only six galaxies also has an extensive hot envelope

© American Astronomical Society • Provided by the NASA Astrophysics Data System

1995ApJ...444..582D

seen with the *ROSAT* PSPC with a temperature similar to the NGC 2300 group but with a higher abundance. The X-ray emitting gas seen in the NGC 4261 is qualitatively similar to that seen in these other groups. The X-rays are peaked near the dominant galaxy, the gas temperature is near 1 keV and the metal abundance is low.

The gas seen in the NGC 4261 group is well fitted with a King profile with a core radius of 1.'68 (26 kpc), a beta value of 0.31, and a central surface brightness of 1.52×10^{-3} counts s^{-1} arcmin^{-2} in the energy range from 0.5 to 2.0 keV. This core radius is unusually small and could be the result of the gas not being in equilibrium with the group potential which could also explain why the gas profile is so flat. Beers & Tonry (1986) suggest that the presence of a cluster core is an artifact of incorrectly identifying the cluster center and that the true profile may be a power law. A power-law fit to the X-ray profile between 3' and 40' does yield a power-law index of ~ 0.9 as predicted by Beers & Tonry. Finally numerical simulations of cluster formation show that the hot gas is more extended than the dark matter (Evrard 1990; Thomas & Couchman 1992; Navarro, Frenk, & White 1994). This is due to the fact that gas that has fallen to the center cannot dissipate enough energy to accurately trace the dark matter. The cool gas in this group may be able to trace the group potential much closer to the center than the hotter gas in clusters. From the observed surface brightness profile and assuming an equation of state for the gas one can relate the observed surface brightness profile to the three-dimensional emissivity of the gas. If we assume that the gas is described by a polytropic equation of state, $T \sim n^{\gamma - 1}$, then the density profile may be written

$$n(r) = n_0[1 + (r/a)^2]^{-\delta}, \quad (1)$$

where

$$\delta \approx \frac{\frac{3}{2}\beta}{1 - 0.20(\gamma - 1)} \quad (2)$$

for $\gamma = 1$ this equation is exact. From equation (1) the mass of gas within a given radius may be written

$$M_{\rm gas}(< r) = 4\pi n_0 a^3 \bar{m} \int^x \frac{y^2\, dy}{(1 + y^2)^{-\delta}}, \quad (3)$$

where a is the core radius, $x = r/a$, $\bar{m}$ is the mass per gas particle. For a spherically symmetric mass distribution in hydrostatic equilibrium the binding mass can be written

$$M_v = 1.92 \times 10^{14}\, \delta y (T/10)_{\rm keV} (a/0.25)_{\rm Mpc}\, x^3 (1 + x^2)^{-(1+\phi)}\, M_\odot \quad (4)$$

where $\phi = \delta(\gamma - 1)$ (Cowie, Henriksen, & Mushotzky 1987). Using the temperature derived above for the gas and assuming that the gas is isothermal, $\gamma = 1$, we find that the total gravitating mass within 40' (620 Kpc) is $1.9^{+0.7}_{-0.4} \times 10^{13}\, M_\odot$.

The gas mass can be obtained using equation (3). Using the normalization from the best-fit spectrum to fix the average gas density and the fitted parameters from the surface brightness profile, we estimate the central gas density to be $6.77^{+0.42}_{-0.47} \times 10^{-4}$ cm^{-3}. Assuming the same core radius, beta value and extent as for the surface brightness fits above, we find a gas mass of $(4.6 \pm 0.3) \times 10^{12}\, M_\odot$ at radii less than 40'. It should be noted that the very flat X-ray profile derived here implies that the gas mass is rising rapidly and that at distances of greater than a few hundred core radii the gas mass will exceed the total mass of the group, so clearly this simple model of the group should not be extended beyond the detected extent of the gas.

We show the radial profiles for the gas and the total gravitating mass for this group in Figure 5. The baryonic mass in the galaxies can be estimated using the mass-to-light ratio and the measured brightness for each galaxy. Table 2 lists the relevant parameters from de Vaucouleurs et al. (1991; RC3) for each of the galaxies within the measured extent of the hot gas. Column (1) lists the name of the galaxy followed by the Hubble type. The position of the galaxy is listed in columns (3) and (4). The heliocentric velocity in km s^{-1} along with the associated error is listed in column (5). The last column gives the total blue magnitude for the galaxy. Note that the group catalog of Nolthenius (1993) has a magnitude cutoff at 14.5, and so we may not be counting all the mass in galaxies. However, this should not introduce a large error in our estimate of the baryonic mass. We assume a mass-to-light ratio of 8.5 for the early-type galaxies (Faber & Gallagher 1979) and 2.6 for the Sc galaxies (Burstein & Rubin 1985). These determinations of the mass-to-light ratio include the dark matter found in these types of galaxies. To be conservative in our estimate of the ratio of baryonic to dark matter we assume that all of the galaxy mass is in baryons. With this we estimate the baryonic mass in the galaxies to be $9.5 \times 10^{11}\, M_\odot$. Using the values derived above

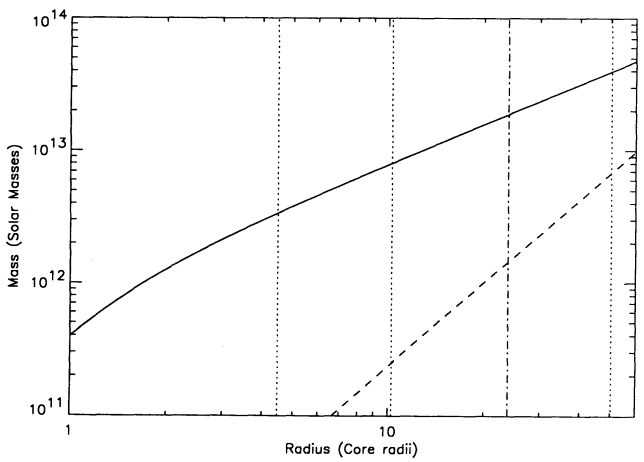

FIG. 5.—Here we show the derived mass profile for the NGC 4261 group. The solid line is the total binding mass. The dashed line below the solid line is the gas mass and the vertical dot-dashed line is the radial limit of the detected X-ray gas. The The vertical dotted lines delimit where the profile of the group gas is 100% ($R = 4.5$), 50% ($R = 10.2$), and 20% ($R = 50.2$) of the measured background. The radial axis is in terms of the core radius of the gas profile. The core radius is 1.'68 (26 kpc).

TABLE 2

N4261 GROUP GALAXIES INSIDE THE GROUP GAS

Object (1)	Type (2)	R.A. (J2000) (3)	Decl. (J2000) (4)	$V_{\rm Hel}$ (5)	M_B (6)
NGC 4259.....	S0	$12^h19^m22^s$	+05°22'33"	2487 ± 30	14.58
NGC 4260.....	SBa	12 19 22	+06 06 00	1886 ± 61	12.70
NGC 4261.....	E2	12 19 23	+05 49 35	2210 ± 14	11.41
NGC 4264.....	SB0	12 19 36	+05 50 50	2650 ± 96	13.70
NGC 4268.....	SB0	12 19 47	+06 17 02	2335 ± 96	13.82
NGC 4270.....	S0	12 19 49	+05 27 52	2323 ± 48	13.07
NGC 4273.....	SBc	12 19 56	+05 20 48	2308 ± 48	12.39
NGC 4281.....	S0	12 20 22	+05 23 12	2685 ± 24	12.25

© American Astronomical Society • Provided by the NASA Astrophysics Data System

1995ApJ...444..582D

for the gas mass, mass in galaxies and the total gravitating mass within 40′ (620 pc), we find that the baryonic matter comprises ~30% of the total mass in this group. Using our derived uncertainties in the gas density and the parameters for the King model we find that the baryonic fraction can range from 20% to 34%. This estimate of the baryonic fraction for the NGC 4261 group is more like that seen in clusters than the other poor groups discussed before. However, the very flat profile we derive for the diffuse gas makes the baryonic fraction very sensitive to the radius at which the masses are calculated.

Our results bring to four the number of groups which have diffuse X-ray gas. *N*-body simulations of group evolution show that the galaxies in these systems can merge to form a single remnant, presumably an elliptical galaxy. The NGC 4261 group can be considered a gaint elliptical galaxy with only dwarf companions, while the galaxies in HCG 62 should form a single elliptical within a few gigayears. The NGC 2300 group contains two roughly equal mass galaxies within 25′ of the center of hot gas distribution. The final state of the NGC 2300 group, whether it forms a single elliptical or remains a loose group, is very sensitive to the orbital parameters of the galaxies. While these groups are very different in their galaxy content, and the mass of X-ray emitting gas ranges from $5.2 \times 10^{11}\ M_\odot$ to $5.0 \times 10^{12}\ M_\odot$, the total gravitating mass varies only from $1\text{–}3 \times 10^{13}\ M_\odot$. The inferred baryonic mass fraction ranges from as little as 6% in the NGC 2300 group to 30% for the NGC 4261 group. Thus, although only a small number of groups have been adequately studied, it is clear that there can be a significant range in some parameters such as gas metallicity and baryonic fraction. Further studies of many more systems will be required to establish the characteristics of a "typical" group of galaxies.

4.2. *The Special Case of NGC 4273*

Our attention was initially drawn to this system by one of the galaxies in the group. This galaxy, NGC 4273, displays a peculiar morphology similar to that of NGC 2276 in the NGC 2300 group, which is characterizied by a curved boundary with a sharp edge along one side of the galaxy. This sharp-edged structure is thought to have been formed by one of two processes: interaction of the ISM of the galaxy with the intergroup gas as the galaxy moves through the group (Condon 1983; Cayette et al. 1990; Kotanyi, van Gorkum, & Ekere 1983), or by tidal interaction with another member of the group.

First, we consider the effects of the intra-group gas on the ISM of NGC 4273. This galaxy lies at a projected distance of 0.47 Mpc (~30′) from the center of the gas distribution. Our best-fit parameters to the gas distribution show that the gas density should drop to $\sim 10^{-7}$ cm^{-3} near NGC 4273. The velocity difference between this galaxy and the group velocity is 191 km s^{-1}. We can write the condition for ram pressure stripping of the gas in a galaxy which has a disk with uniform surface density, a radius of r_D, a mass M_D, moving at σ_r through the intracluster gas as

$$\left(\frac{n_g}{10^{-3}\ \mathrm{cm}^{-3}}\right)\left(\frac{\sigma_r}{10^3\ \mathrm{km\ s}^{-1}}\right)^2 \gtrsim 3\left(\frac{M_D}{10^{11}\ M_\odot}\right)^2 \times \left(\frac{r_D}{10\ \mathrm{kpc}}\right)^{-4}\left(\frac{M_{\mathrm{ISM}}}{0.1\ M_D}\right) \quad (5)$$

Sarazin (1986, eq. 5.114). Here n_g is the number density of particles in the intracluster medium and M_{ISM} is the mass of the interstellar medium in the disk. From this we can see that the group gas is much too tenuous to perturb the ISM of NGC 4273 except in the very outer parts. An alternate scenario would be to have NGC 4273 interacting with a local enhancement of gas perhaps associated with the small clump of galaxies surrounding NGC 4273. Examination of the X-ray emission in that portion of the PSPC field does not reveal any such local enhancement.

Given that the group gas is not a likely candidate for the odd morphology for NGC 4273, the other possible origin for this distorted morphology is a tidal encounter with another galaxy. Of the eight galaxies nearest NGC 4261, five, including NGC 4273, form a small clump centered ~30′ from NGC 4261. None of the other galaxies appear tidally disturbed. It is unlikely that the morphology of NGC 4273 is from a past merger and the companion has merged with the larger galaxy. Only the outer disk appears disturbed while the inner part appears relatively normal.

NGC 4273 lies at a current projected distance of 0.47 Mpc from NGC 4261, so that the current tidal effects are minimal. For the tidal hypothesis to work NGC 4273 must have been much closer to NGC 4261 in the past. However, even if NGC 4273 has a close encounter with NGC 4261 it is difficult to understand the persistence of the distorted morphology. Differential rotation should blur any sharp boundary caused by an encounter in less than a galactic rotation period. The observed velocity difference between NGC 4261 and NGC 4273 is only ~100 km s^{-1}. At NGC 4273's projected distance from NGC 4261 and the observed velocity difference, it would have taken NGC 4273 $\sim 5 \times 10^9$ yr to reach that distance, assuming zero separation in the past. The true space velocity of NGC 4273 can be much higher but if it is bound to the group it must have a velocity less than ~600 km s^{-1}. This would reduce the allowed time between the proposed tidal encounter to slightly less that 10^9 yrs. Either timescale would allow for several galactic rotations which would erase any sharp features created by tidal forces.

This only leaves the possibility of a tidal interaction with other members of the group. No other galaxy in this group shows such a distorted morphology; however, if NGC 4273 interacted with a less massive companion, it may have been disrupted leaving little evidence of the original encounter.

5. CONCLUSIONS

We have found X-ray emitting gas in the central 0.6 Mpc of the NGC 4261 group. We see evidence for this gas in the surface brightness distribution and in the extracted spectrum. The gas is well fitted by a Raymond-Smith plasma model with a temperature $0.85^{+0.21}_{-0.16}$ keV and an upper limit on the abundance of 0.08 times the solar value at 90% confidence. This X-ray emission from the group extends to at least 620 kpc (40′) and the surface brightness is well fitted with a modified King profile with a core radius of 26 kpc (1.′68) and a beta value of 0.31. This value of beta corresponds to an unusually flat profile. The luminosity of this gas is 5.5×10^{41} ergs s^{-1}.

The total gravitating mass of the group can be estimated by assuming that the X-ray emitting gas is trapped in the potential well of the group and has had time to reach hydrostatic equilibrium. This implies a total mass of $1.9 \times 10^{13}\ M_\odot$. The baryonic mass from the hot gas and the galaxies within the extent of the thermal plasma is 30% of the total mass. This baryonic fraction is similar to those seen in much richer clusters of galaxies while the low metal abundance is much more like that seen in other poor groups. These data along with previously

© American Astronomical Society • Provided by the NASA Astrophysics Data System

1995ApJ...444..582D

published results for the NGC 2300 group, HCG 62 and the NGC 5044 group indicate that the baryonic fraction in groups can cover a wide range of values and that many more groups must be analyzed before a "typical" group can be defined.

While the distorted morphology of NGC 4273 might be attributed to its ISM interacting with gas in the NGC 4261 group, the velocity of NGC 4273 and our measurements of the density of the group gas suggest that that the diffuse gas in the group is much too tenuous to significantly disturb the galaxy. With this in mind we conclude that the distorted morphology seen in NGC 4273 is more likely to be a result of a tidal encounter with another member of the NGC 4261 group.

The *ROSAT* All Sky Survey data is courtesy of MPE Garching, Germany. M. B. and D. M. W. would like to acknowledge the support of *ROSAT* grant NAG 5-2312 and NASA contract NAS8-39073. We would like to thank our anonymous referee for their helpful comments.

REFERENCES

Bahcall, N. A., Harris, D. E., & Rood, H. J. 1984, ApJ, 284, L29
Beers, T. C., & Tonry, J. L. 1986, ApJ, 300, 557
Biermann, P., & Kronberg, P. P. 1983, ApJ, 268, 69
Biermann, P., Kronberg, P. P., & Madore, B. F. 1982, ApJ, 256, L37
Burstein, D., & Rubin, R. 1985, ApJ, 297, 423
Cayette, V., van Gorkum, J. H., Balkowski, C., & Kotanyi, C. 1990, AJ, 100, 604
Condon, J. J. 1983, ApJS, 53, 459
Cowie, L. L., Henriksen, M. J., & Mushotzky, R. F. 1987, ApJ, 317, 593
de Vaucouleurs, G., de Vaucouleurs, A., Corwin, H. G., Buta, R. J., Paturel, G., & Fouqué, P. 1991, Third Reference Catalogue of Bright Galaxies (Austin: Univ. of Texas) (RC3)
David, L. P., Jones, C., Forman, W., & Daines, S. 1994, ApJ, 428, 544
Evrard, A. E. 1990, in Clusters of Galaxies, ed. M. Fitchett & W. Oegerle (Cambridge: Cambridge Univ. Press)
Faber, S. M., & Burstein 1988, in Proc. Pontifical Acad. Sciences Study Week, No. 27, Large-Scale Motions in the Universe (Princeton: Princeton Univ. Press), 116
Faber, S. M., & Gallagher, J. S. 1979, ARA&A, 20, 547
Hickson, P. 1982, ApJ, 255, 382
Jones, C., & Forman, W. 1984, ApJ, 276, 38
Kotanyi, C., van Gorkum, J. H., & Ekers, R. D. 1983, ApJ, 273, 7
Mulchaey, J. S., Davis, D. S., Mushotzky, R. F., & Burstein, D. 1993, ApJ, 404, L9
Navarro, J. F., Frenk, C. S., & White, S. D. M. 1994, preprint
Nolthenius, R. 1993, ApJS, 85, 1
Ponman, T. J., & Bertram, D. 1993, Nature, 363, 51
Raymond, J. C., & Smith, B. W. 1977, ApJ, 35, 419
Sarazin, C. L. 1986, Rev. Mod. Phys., 58, 1
Snowden, S. L., McCammon, D., Burrows, D. N., & Mendenhall, J. A. 1994, ApJ, 424, 714
Stark, A. A., Gammie, C. F., Wilson, R. W., Bally, J., Linke, R. A., Heiles, C., & Hurwitz, M. 1992, ApJS, 79, 77
Thomas, P. A., & Couchman, H. M. P. 1992, MNRAS, 275, 11
Worrall, D. M., & Birkinshaw, M. 1994, ApJ, 520, 134

© American Astronomical Society • Provided by the NASA Astrophysics Data System